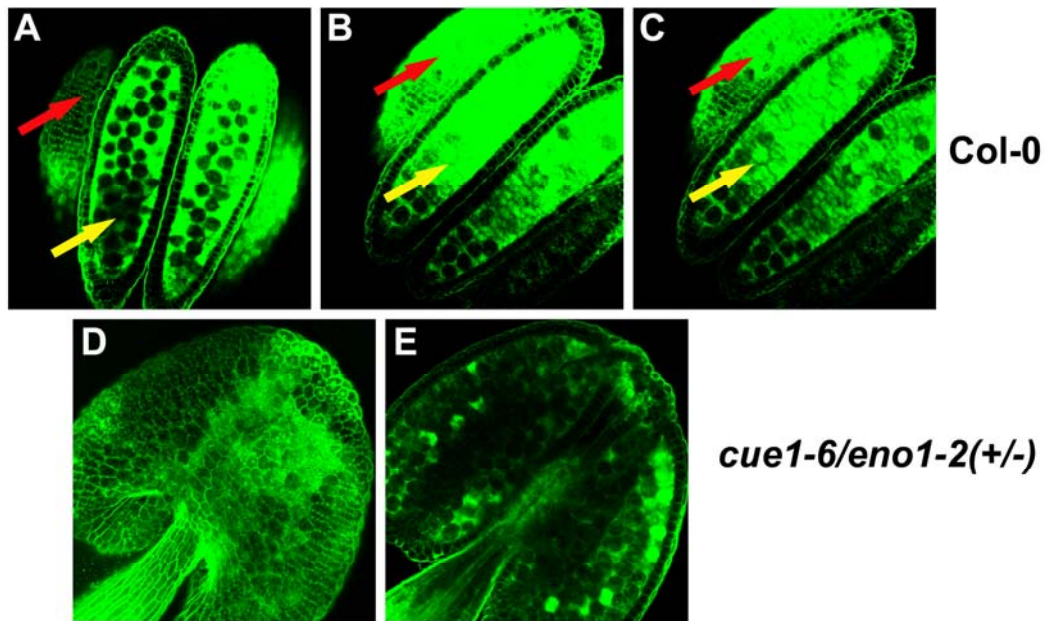


Supplemental Figure 1. Comparison of the shoot and root phenotypes of heterozygous *eno1* mutants in the homozygous *cue1* background (*ccEe*) with *cue1* single mutants.

(A) Comparison of shoot and silique phenotypes of 7 week old *cue1-6* mutant (1) with the *cue1-6/eno1-2(+/-)* double mutant showing varying degrees of shoot retardation and aberrant silique development (2-6). The scale bar represents 14 cm.

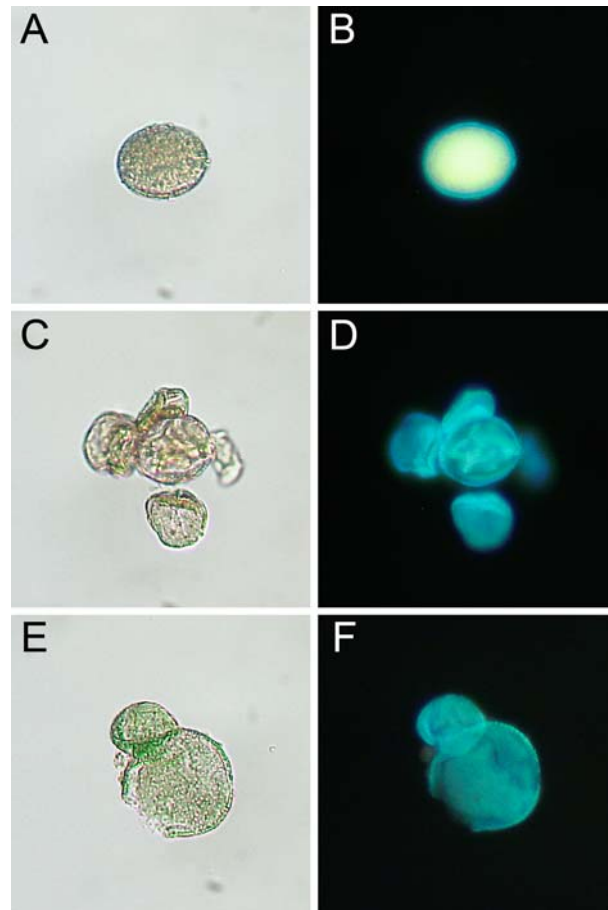
(B) Phenotypic appearance of *cue1-6* plants compared to the heterozygous *eno1* mutant in the homozygous *cue1* background (*cue1-6/eno1-2(+/-)*) grown for three weeks on MS agar.



Supplemental Figure 2. Confocal microscopic images of pollen sacs from Col-0 wild-type plants and heterozygous *ccEe* double mutants. Autofluorescence of phenolic compounds was captured at an emission of $\lambda = 488$ nm following excitation at $\lambda = 500$ - 550 nm.

(A-C) Stamen of wild-type plants (Col-0), showing both the interior (yellow arrow) and the surface (red arrow) of the pollen sac.

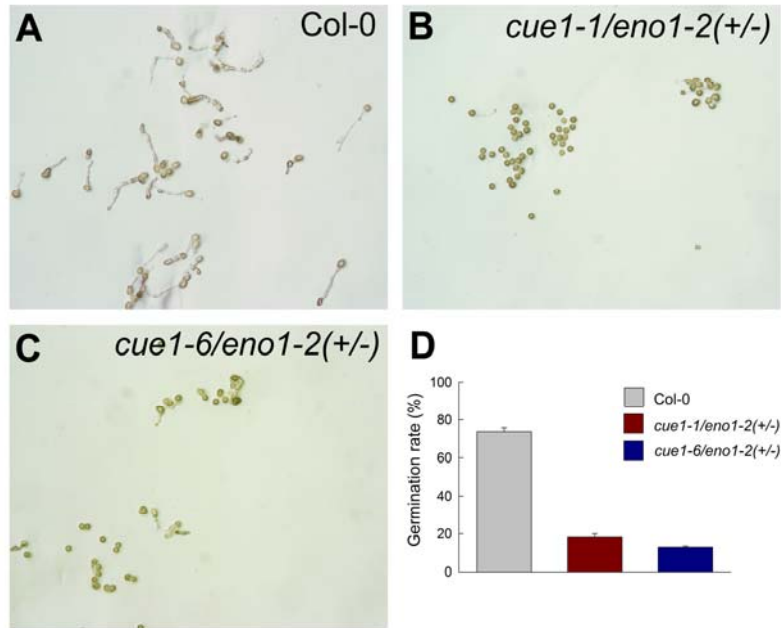
(D, E) Stamen of *cue1-6/eno1-2(+/-)* showing the surface (**D**) and the interior (**E**) of the pollen sac.



Supplemental Figure 3. Autofluorescence of pollen from a wild-type plant and a heterozygous *eno1* mutants in the homozygous *cue1* background (*ccEe*). The fluorescence was enhanced with DPBA (excitation: $330\text{ nm} > \lambda < 380\text{ nm}$, emission: $\lambda > 420\text{ nm}$). The left and right panel represents bright field and fluorescence images, respectively.

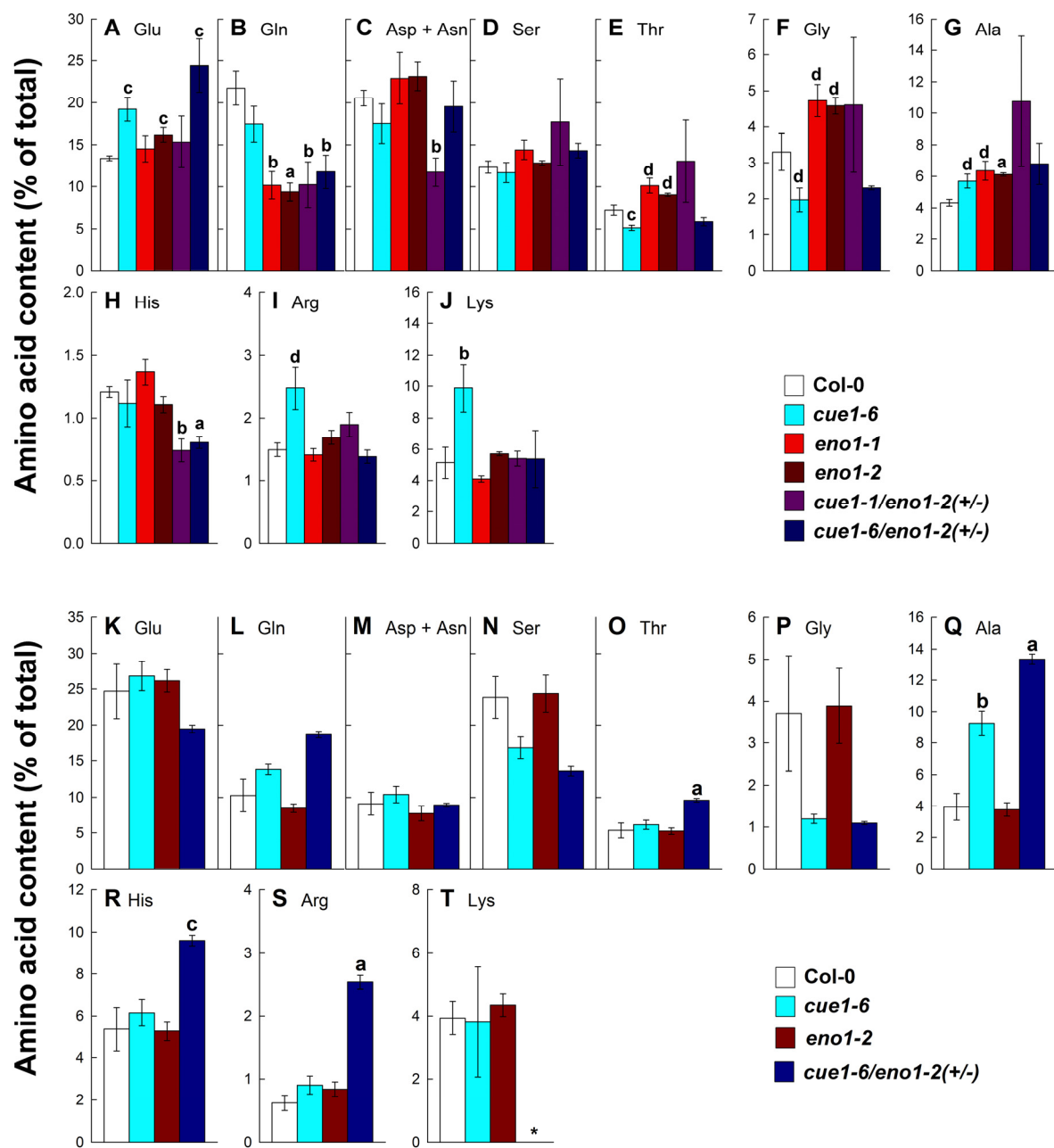
(A, B) Pollen grain of a wild-type plant (Col-0).

(C-F) Pollen grains of the *cue1-1/eno1-2(+/-)* double mutant.

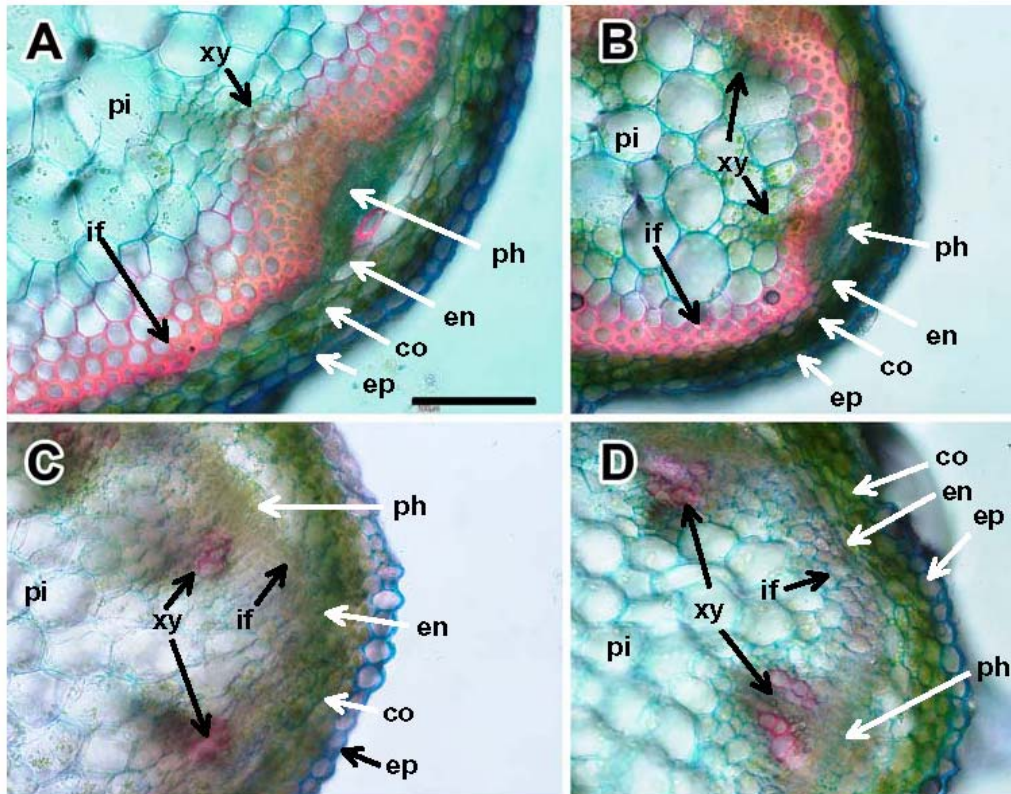


Supplemental Figure 4. Comparison of pollen germination rates between *A. thaliana* wild-type (Col-0) and the *ccEe* plants with alleles *cue1-1/eno1-2(+/-)* and *cue1-6/eno1-2(+/-)*. Pollen were germinated at 25°C in closed Petri dishes and the germination rates assessed after 6h. For (D) five batches each of 100 pollen per line were counted. The data represent the mean \pm SE (n = 5)

- (A) Germination of pollen from Col-0.
- (B) Germination of Pollen from *cue1-1/eno1-2(+/-)*.
- (C) Germination of Pollen from *cue1-6/eno1-2(+/-)*.
- (D) Relative germination rates of pollen from Col-0, *cue1-1/eno1-2(+/-)*, and *cue1-6/eno1-2(+/-)*.

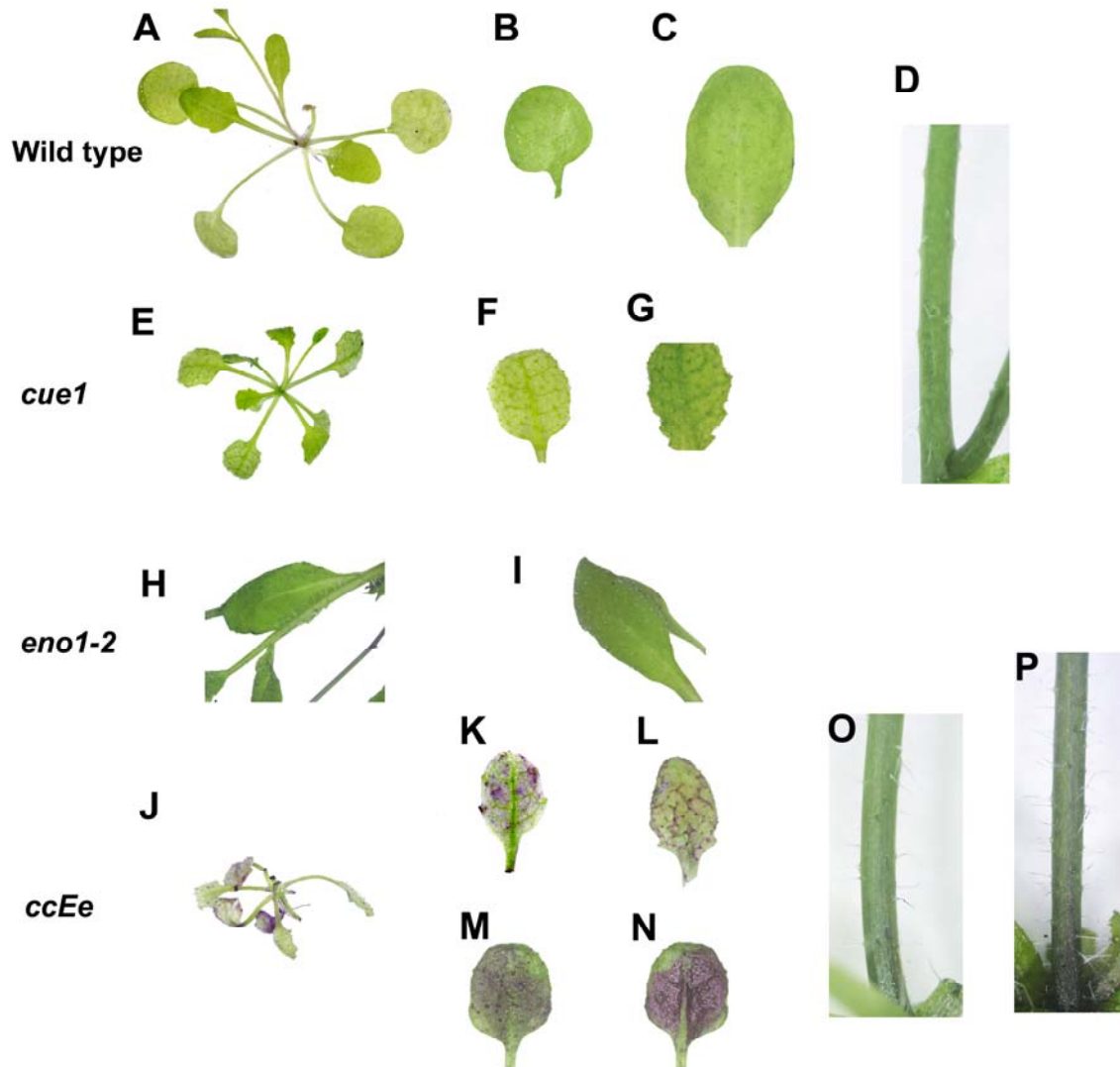


Supplemental Figure 5. Relative contents of free amino acids extracted from flower buds (A-J) or rosette leaves (K-T) of the wild type (Col-0), the *cue1-6* and *eno1* single mutants as well as the heterozygous *eno1* mutants in the homozygous *cue1* background (*ccEe*). The relative contents of amino acids were expressed as a percentage fraction of the total amino acid content estimated from the sum of all recognized proteinogenic amino acid after separation by HPLC (compare Figure 6, A and H). The data represent the mean \pm SE of $n = 5$ (A-J) or $n = 3$ (K-T) independent experiments. Statistical significance of differences between the parameters were assessed by the Welch-test with probability values of $P < 0.001$ (a), $P < 0.01$ (b), and $P < 0.05$ (c) indicated above the respective bars. The star in (T) indicates that Lys could not be determined in leaves of *cue1-6/eno1-2(+/-)*.



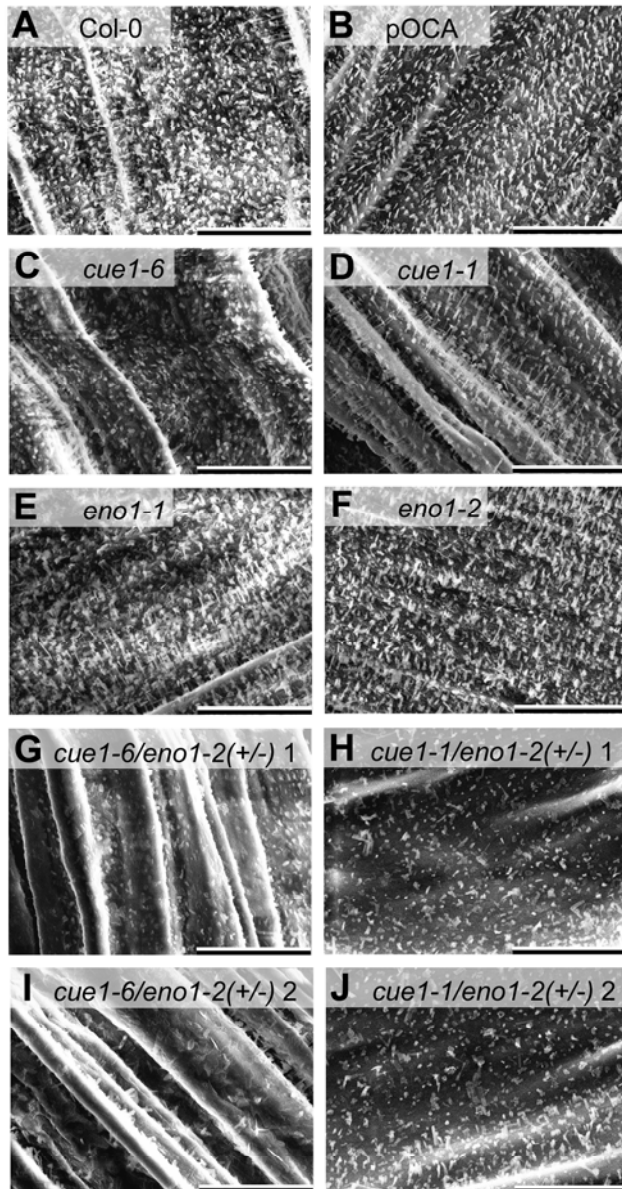
Supplemental Figure 6. Cross sections of the inflorescence stem of heterozygous *eno1* mutants in the homozygous *cue1* background (*ccEe*) compared to wild-type and *cue1* plants stained with ACF to visualize lignin (red) or cellulose (blue) in cell walls. ep, epidermis; co, cortex (chlorenchyma); if, interfascicular cells (sclerenchyma); en, endodermis; ph, phloem; xy, xylem; pi, pith. The bar in **A** represents 100 μm and refers to all subfigures.

- (A)** Col-0.
- (B)** *cue1-6*.
- (C)** *cue1-6/eno1-2(+/-)*.
- (D)** *cue1-1/eno1-2(+/-)*.



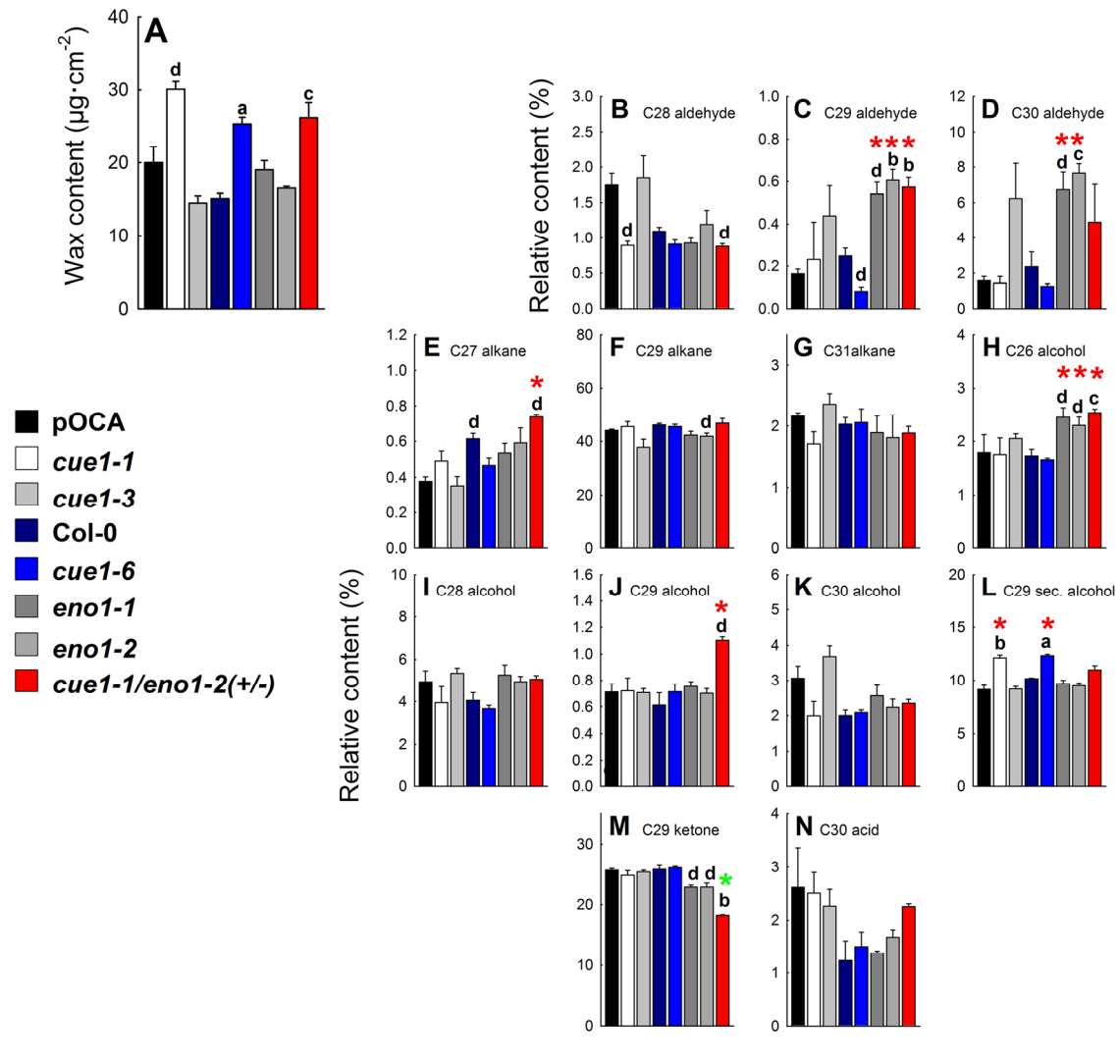
Supplemental Figure 7. Typical Toluidine Blue (TB) staining for cuticle integrity of arial parts of the heterozygous *eno1* mutant in the homozygous *cue1* background (*ccEe*) compared to the wild type (pOCA = ecotype Bensheim, Col-0), the *cue1* and *eno1* single mutants grown for three weeks in a greenhouse.

(A) pOCA rosette, (B) pOCA leaf, (C) Col-0 leaf, (D) Col-0 inflorescence stem, (E) *cue1-1* rosette, (F) *cue1-1* leaf, (G) *cue1-6* leaf. (H) excerpt of a *eno1-2* rosette, (I) *eno1-2* leaf, (J) *cue1-1/eno1-2(+/-)* rosette, (K, L) *cue1-1/eno1-2(+/-)* leaf, (M) *cue1-6/eno1-2(+/-)* leaf adaxial side, (N) *cue1-6/eno1-2(+/-)* leaf abaxial side, (O, P) *cue1-6/eno1-2(+/-)* inflorescence stems.



Supplemental Figure 8. SEM images of epicuticular wax crystals of inflorescence stems of *A. thaliana* wild type (Col-0, pOCA = ecotype Bensheim) as well as mutant alleles of *cue1*, *eno1* and *ccEe*. The scale bars indicate 20 μ m.

- (A) Col-0.
- (B) pOCA.
- (C) *cue1-6*.
- (D) *cue1-1*.
- (E) *eno1-1*.
- (F) *eno1-2*.
- (G, I) *cue1-6/eno1-2(+/-)*, different plants (1, 2) of the same line.
- (H, J) *cue1-1/eno1-2(+/-)*, different plants (1, 2) of the same lines.



Supplemental Figure 9. Epicuticular wax analysis of inflorescence stems of *A. thaliana* wild-type (pOCA = ecotype Bensheim, Col-0) as well as alleles of *cue1*, *eno1* and *cue1-1/eno1-2(+/-)*. Red and green stars represent compounds, which are either over- or underrepresented, respectively, in the individual lines referred to the wild type. Statistical significance of differences between the parameters were assessed by the Welch-test with probability values of $P < 0.001$ (a), $P < 0.01$ (b), $P < 0.02$ (c), $P < 0.05$ (d) indicated above the respective bars.

(A) Total epicuticular wax content expressed per stem surface area.

(B-P) Relative contents of wax components as separated by GC/MS expressed as percent of total wax content in the epicuticular layer.

(B-D) C28, C29, and C30 aldehydes.

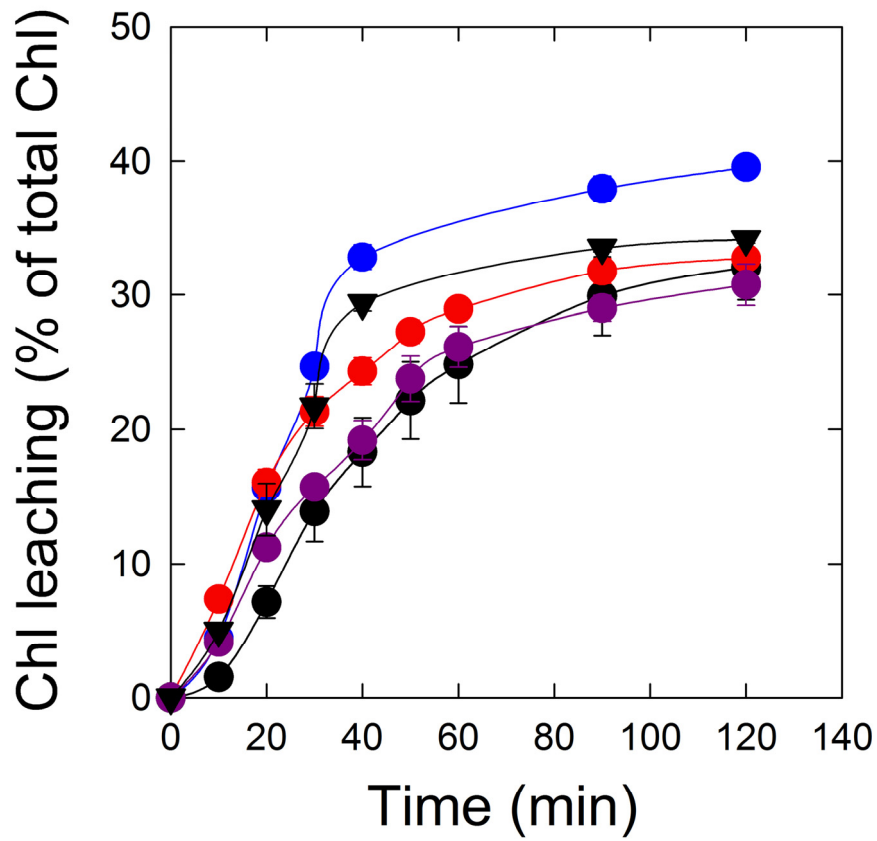
(E-G) C27, C29, and C31 alkanes.

(H-K) C26, C28, C29, and C30 alcohols.

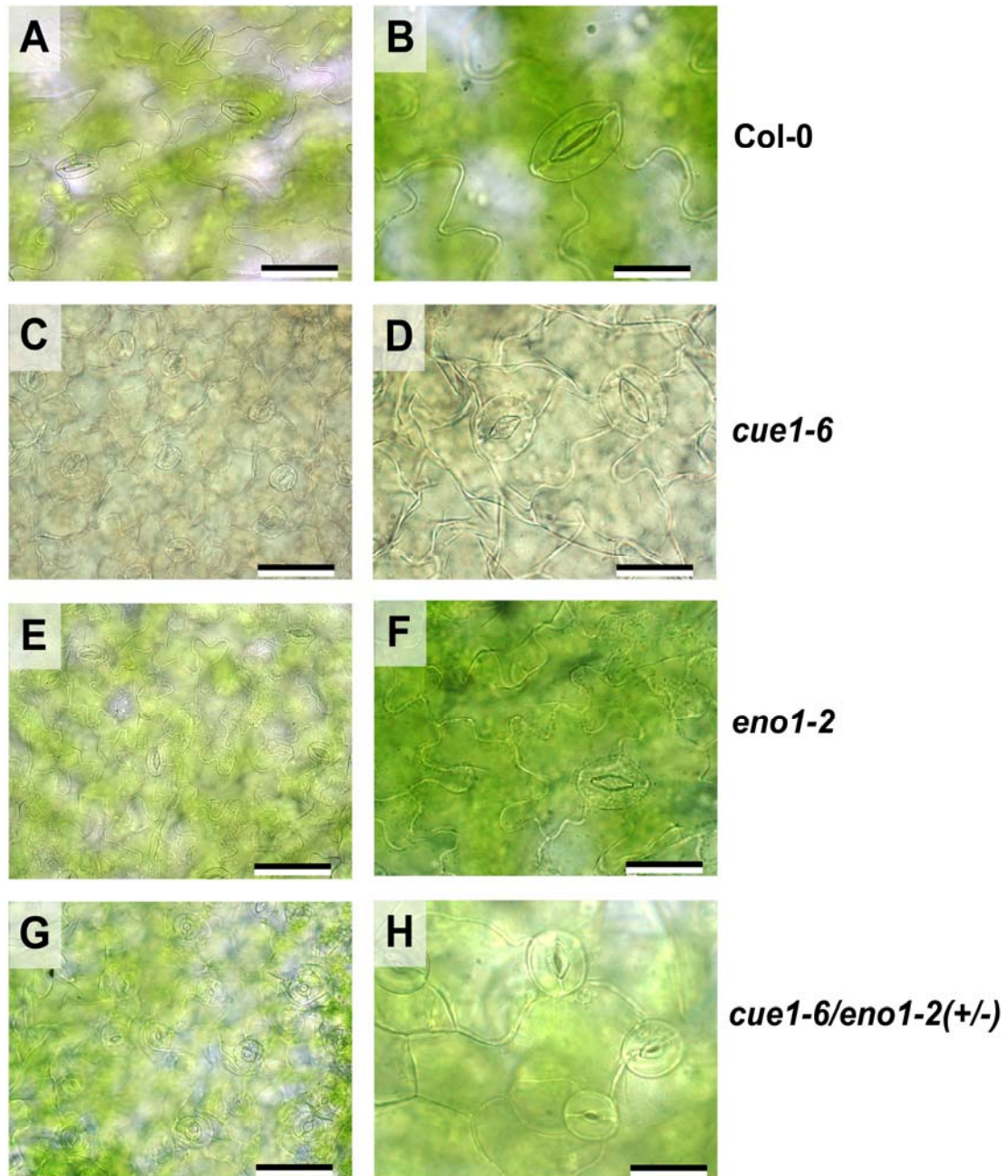
(L) C29 secondary alcohol.

(M) C29 ketone.

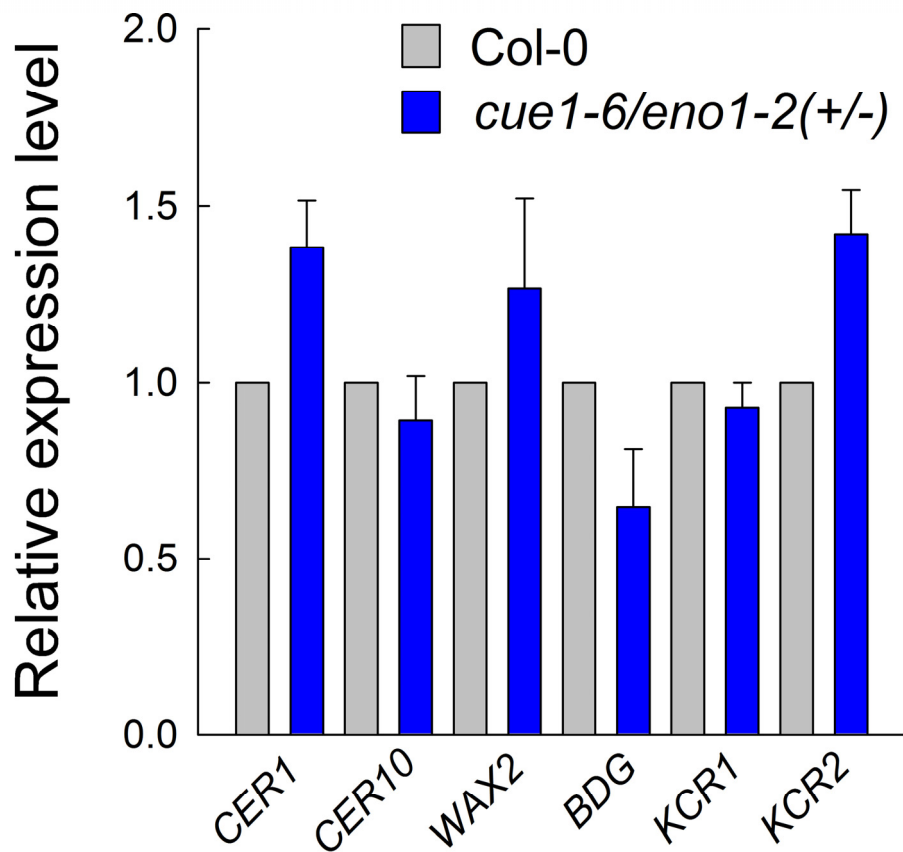
(N) C30 acid.



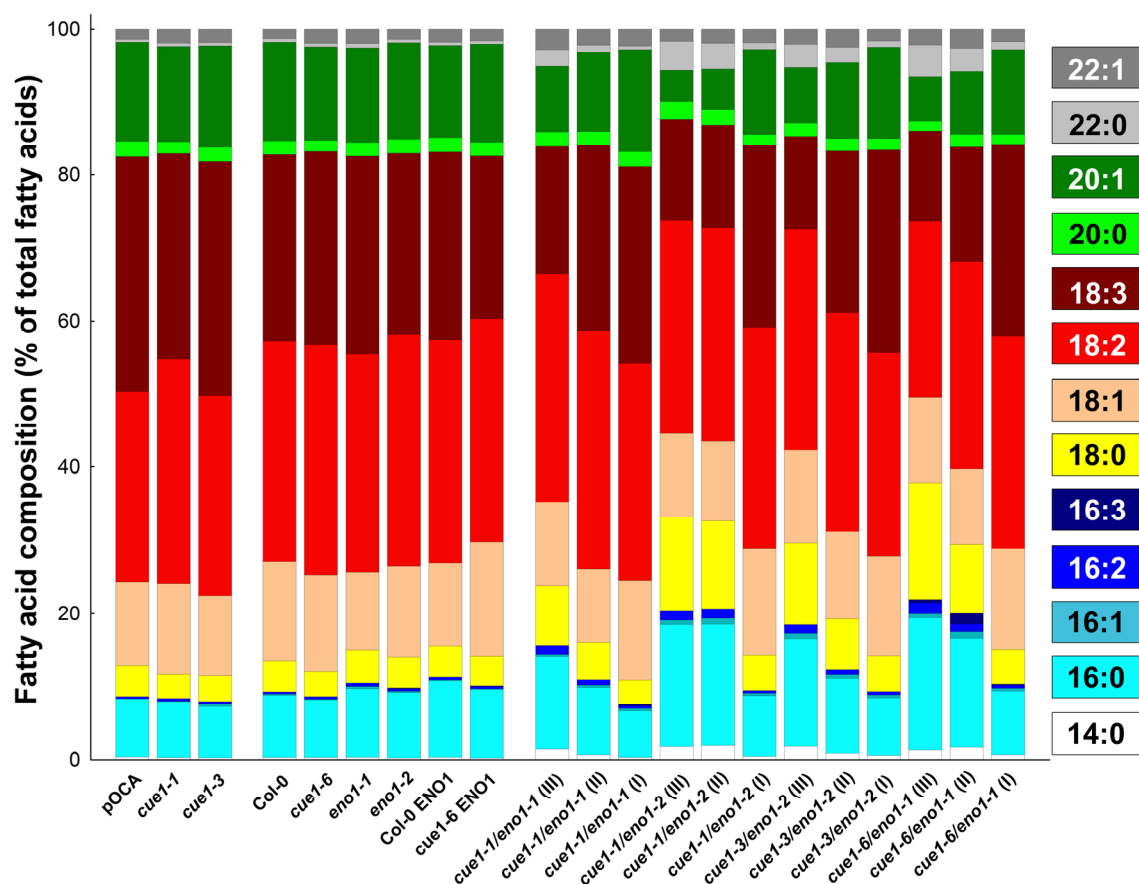
Supplemental Figure 10. Chl leaching experiment with cut leaves of 6 week old Col-0 (●, ▲), *eno1-2* (●), *cue1-6* (●) and *cue1-6/eno1-2(+/-)* (●). Chl contents are referred to the percentage of total Chl contents in the individual sample. The data represent the mean \pm SE of three independent experiments. Note that for Col-0 two independent batches of plants were used.



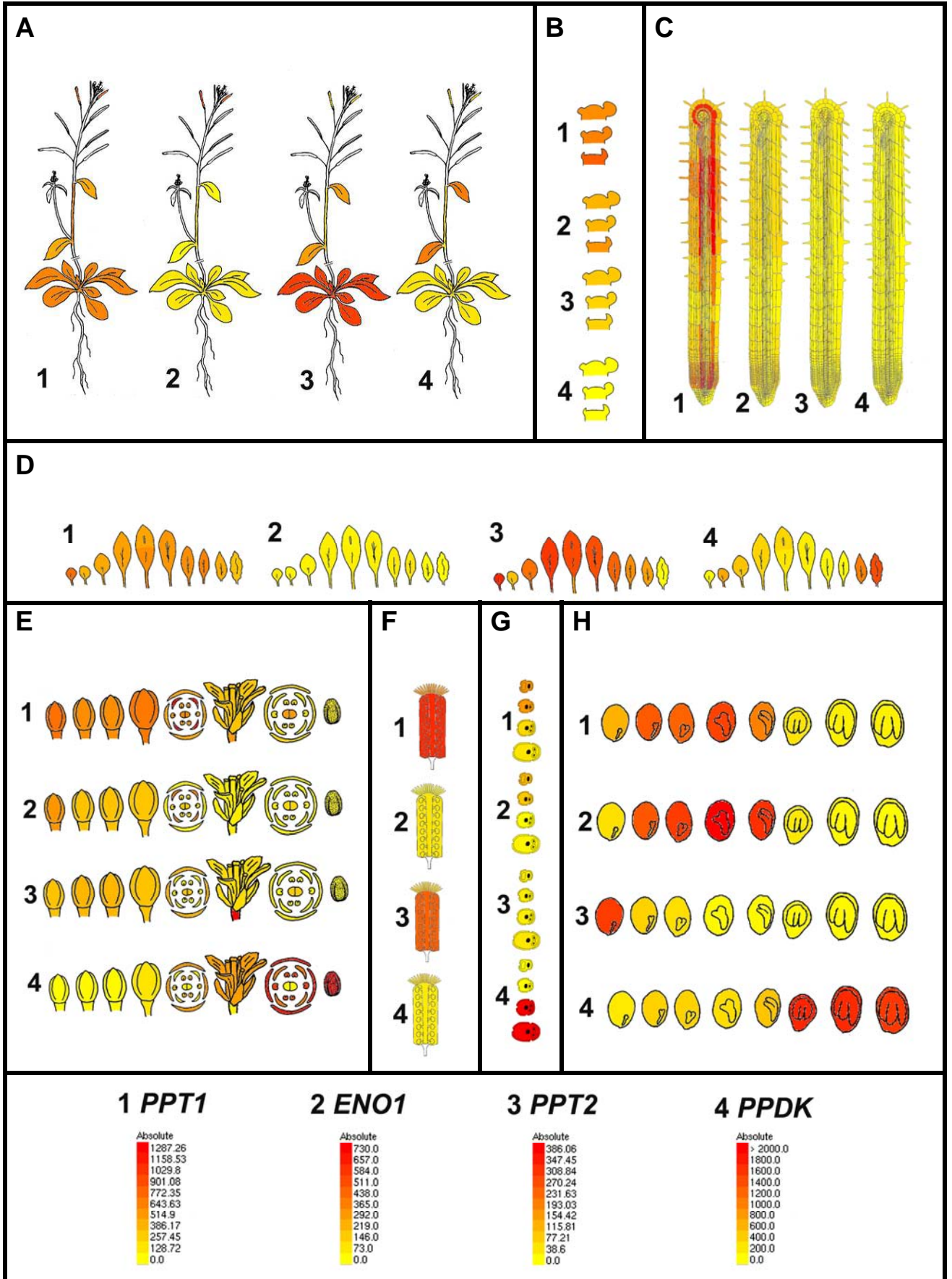
Supplemental Figure 11. Light microscopic images showing the distribution of stomata as well as the phenotypes of stomatal guard cells on the adaxial surface of rosette leaves of the wild type (Col-0) (**A**, **B**), the *cue1-6* (**C**, **D**) and *eno1-2* (**E**, **F**) single mutants as well as in the heterozygous *eno1-2* mutant in the homozygous *cue1-6* background (*cue1-6/eno1-2[+/-]*) (**G**, **H**). The bars represent 50 μm and 20 μm for (A, C, E, G) and (B, D, F, H), respectively.



Supplemental Figure 12. Relative transcript levels of genes involved in cuticular wax biosynthesis in *cue1-6/eno1-2(+/-)* compared to the wild type. Expression levels were assessed by qRT-PCR and normalized for the expression of *Actin2*. The bars represent the mean \pm SE of three experiments.



Supplemental Figure 13 Relative composition of saturated and desaturated fatty acids determined by gas chromatography after derivatization to fatty acid methyl esters. The fatty acid composition was determined on single seeds ($n = 5-10$) and referred to the total lipid content of the individual samples. The single mutants *cue1-1*, *cue1-3*, *cue1-6*, *eno1-1*, and *eno1-2* were compared to their respective wild-type (Col-0) or control plants (pOCA). For the wild-type as well as *cue1-6* plants overexpressing *ENO1*, data of the lines Col-0 ENO1 (A) and Col-0 ENO1 (C) as well as *cue1-6* ENO1 (4) and *cue1-6* ENO1 (5) were grouped. The roman numbers for the heterozygous *eno1* mutants in the homozygous *cue1* background represent measurement on individual class I, class II and class III seeds.



Supplemental Figure 14. Spatial and developmental expression profiles of genes involved in PEP delivery to plastids (i.e. 1, *PPT1*; 2, *ENO1*; 3, *PPT2* and 4, *PPDK*). The pictures were extracted from the eFP-browser platform (<http://bar.utotonto.ca/efp/cgi-bin/efpWeb.cgi>; Winter et al., 2007) and are based on microarray analyses.

- (A) Rosette and cauline leaves as well as siliques on a whole plant level.
- (B) Shoot apical meristem.
- (C) root.
- (D) Rosette leaf development.
- (E) Flower development.
- (F) Carpels.
- (G) Microsporophyte development.
- (F) Embryo development.

In the lower panel the absolute expression levels of the individual genes and the corresponding color scales are shown. For more detailed information on the individual experiments please refer to (<http://bar.utotonto.ca/efp/cgi-bin/efpWeb.cgi>).

Supplemental Table 1. Genotype analysis of the F2 generation of crosses between *cue1* and *eno1* mutants.

A Expected Mendelian distribution of genotypes in the segregating F2 generation of crosses between *cue1* and *eno1* mutants. C and E represent the wild type and c and e the mutated loci of *ENO1* and *CUE1*, respectively. **B** Distribution of genotypes in the segregating F2 population of crosses between *cue1-1* (male) and *cue1-6* (male) with *eno1-2* (female) as well as the invers cross between *eno1-2* (male) and *cue1-1* (female). The right panel shows the expected Mendelian distribution of genotypes. **C** Male and female transmission efficiency (TE) of the *eno1* and *cue1* mutations. TE was estimated from reciprocal crosses of *cue1-1* and *eno1-2* mutants in the segregating F2 generation obtained from the self-crossed F1 generation. TE is defined as 'number of mutated alleles' / number of total alleles x 100'. For a typical Mendelian inheritance a TE of 50% for each gametophyte would be expected.

A

Genotype	CE	Ce	cE	ce
CE	CCEE	CCEe	CcEE	CcEe
Ce	CCeE	CCee	CceE	Ccee
cE	cCEE	cCEe	ccEE	ccEe
ce	cCeE	cCee	cceE	ccee

B

Genotype	<i>cue1-1/eno1-2(+/-)</i> (75 plants)	<i>eno1-2/cue1-1(+/-)</i> (72 plants)	<i>cue1-6/eno1-2(+/-)</i> (74 plants)	Expected distribution (%)
CCEE	23 (31)	15 (21)	4 (5)	6.25
CCee	5 (7)	7 (10)	13 (18)	6.25
CCEe	8 (11)	12 (17)	20 (27)	12.5
CcEE	31 (41)	17 (24)	7 (10)	12.5
CcEe	2 (3)	10 (14)	20 (27)	25
Ccee	2 (3)	4 (6)	0 (0)	12.5
ccEe	2 (3)	4 (6)	4 (5)	12.5
ccEE	3 (4)	6 (8)	5 (7)	6.25
ccee	0 (0)	0 (0)	0 (0)	6.25

C

Parental genotypes	Male TE (%)	Female TE (%)
ENO1 x <i>eno1-2</i>	31.3	16.7
PPT1 x <i>cue1-1</i>	28.7	31.3

Male and female transmission efficiencies of the *cue1* and *eno1* mutation were diminished in segregating ccEe plants

The crossing diagram in Supplemental Table 1A shows the expected distribution of genotypes providing that a Mendelian inheritance is applicable. As shown in Supplemental Table 1B, the segregation pattern of the *cue1-1* x *eno1-2* plants were far from a Mendelian distribution and exhibited a high percentage of plants with a wild-type genotype (31%) and plants heterozygous for the mutation in the *PPT1* gene (41%). All other genotypes were severely diminished in number. As expected, no double homozygous plants could be detected. Interestingly, the segregation pattern of the reciprocal cross (i.e. *eno1-2* male with *cue1-1* female) exhibited a distribution, which was closer to the expected numbers of genotypes according to a Mendelian inheritance. In particular, numbers of the ccEe, CcEE, CCEe and CCee genotypes were similar to the expected distribution, suggesting differences in the male and female transmission efficiencies (TE) for the *cue1* and *eno1* mutation in the reciprocal cross. For the mutation in the *PPT1* gene, both female and male TE were similar (30%), but lower than the expected value of 50% for each gametophyte (Supplemental Table 1C). In contrast, the female TE for the mutation in the *ENO1* gene was about half (16.7%) compared to the male TE (31.3%), suggesting that a lesion of *ENO1* in the background of

the homozygous *cue1* mutant has a much stronger effect than a lesion in the *PPT1* gene in the homozygous *eno1* background, in particular on embryo sac development. This view was supported by the observation that *Ccee* plants lack any growth phenotype in the vegetative state and a lower percentage of seeds aborted, i.e. 10.22 ± 1.19 % and 13.3 ± 2.68 % for the *cue1-1* x *eno1-2* and *eno1-2* x *cue1-1* crosses, respectively, compared to more than 80% seed abortion in the *ccEe* plants (Table 2; main manuscript). Likewise the percentage of non-viable pollen of *Ccee* plants was reduced to 9.0 ± 1.0 % and 12.4 ± 1.2 % in *cue1-1* x *eno1-2* and *eno1-2* x *cue1-1* crosses, respectively, compared to 35% in the *ccEe* plants (Table 2, main manuscript). Interestingly, crosses of *cue1-6* and *eno1-2* also exhibited a segregation pattern for some of the genotypes of the F2 generation (i.e. CCEE, *ccEe*, CcEE and CcEe) closer to a Mendelian distribution. However, it is not clear as to why these differences in genotype distributions between the individual *cue1* alleles occur. It is conceivable that these differences are based on the individual ecotypes (i.e. Bensheim [pOCA] for *cue1-1* and Col-0 for *cue1-6*). Moreover, the lesion of the *PPT1* gene in *cue1-6* is caused by a point mutation leading to a translational stop codon, whereas parts of chromosome 5 are deleted in *cue1-1*, which not only affects *PPT1* but also at least 5 additional expressed genes in the vicinity of *PPT1* (unpublished data).

Supplemental Table 2. Content of flavonoids in flowers of *A. thaliana* wild-type plants, *cue1* and *eno1* mutant alleles and heterozygous *eno1-2* mutants in the homozygous *cue1-6* background.

Plant line	Flavonoid content (nmol·g ⁻¹ fw)
pOCA	6.51 ± 0.30
<i>cue1-1</i>	9.31 ± 0.42 ^a
<i>cue1-3</i>	10.82 ± 1.84
Col-0	9.64 ± 0.59
<i>cue1-6</i>	6.13 ± 0.60 ^b
<i>eno1-1</i>	8.01 ± 0.23 ^c
<i>eno1-2</i>	8.57 ± 0.98
<i>cue1-6/eno1-2(+/-)</i>	5.56 ± 0.56 ^a

The data represent the mean value ± SE of n = 5 samples each. Statistical significance of differences between the parameters was assessed by the Welch-test with probability values of P < 0.001 (a), P < 0.01 (b), P 0.05 (c).

Supplemental Table 3. Detailed tissue and development specific expression profiles of genes involved in PEP provision to plastids (i.e. *PPT1*, *ENO1*, *PPT2* and *PPDK*), as well as pyruvate synthesis in plastids (*PKp1,2,3*; *ME4*) and the cytosol (*PKc*) in generative (**A**) and vegetative (**B**) tissues. The data were extracted from the eFP-browser platform (<http://bar.utotonto.ca/efp/cgi-bin/efpWeb.cgi>; Winter et al., 2007) and are based on microarray analyses.

A

GENES (AGI code)

Generative tissues	<i>PPT1</i> At5g33320		<i>ENO1</i> At1g74030		<i>PPT2</i> At3g01550		<i>PPDK</i> At4g15530		<i>PKp1</i> At3g22960		<i>PKp2</i> At5g52920		<i>PKp3</i> At1g32440		<i>PKc</i> At5g08570		<i>PKc</i> At5g63680		<i>PKc</i> At5g56350		<i>ME4</i> At1g79750	
	E	SD	E	SD	E	SD	E	SD	E	SD	E	SD	E	SD	E	SD	E	SD	E	SD	E	SD
Flowers																						
Flower Stage 9	717.4	5.2	296.3	5.2	89.5	2.6	3.8	2.3	532.8	2.7	510.2	32.5	95.2	6.1	215.9	4.3	141.2	1.1	236.2	1.1	466.5	3.8
Flower Stage 10/11	566.9	50.6	169.4	8.1	109.1	6.4	59.6	2.0	481.8	8.1	496.8	30.3	85.8	6.2	248.7	2.4	137.8	4.4	209.2	13.78	530.9	17.9
Flower Stage 12	681.6	39.0	164.8	6.4	89.6	9.2	208.9	13.2	534.2	19.8	513.1	8.5	95.5	2.9	301.6	16.3	164.3	6.7	276.8	10.68	512.3	25.0
Flower Stage 12, Carpels	591.6	31.5	150.6	11.4	84.8	8.4	10.7	3.5	560.8	19.0	489.6	4.1	63.9	3.6	255.2	8.1	210.4	1.9	292.2	5.26	513.7	7.4
Flower Stage 12, Petals	1287.3	89.3	379.8	8.3	16.0	1.7	28.8	0.8	1042.5	17.6	1084.3	41.9	118.6	7.0	354.2	8.5	181.7	2.9	325.1	23.86	726.2	12.7
Flower Stage 12, Sepals	456.6	28.1	38.9	1.8	113.3	3.7	831.6	57.7	253.7	5.3	197.1	6.7	121.1	6.7	439.4	17.8	136.4	11.5	456.8	8.87	341.7	7.6
Flower Stage 15	297.4	20.0	55.5	5.8	55.0	2.4	758.2	17.0	368.8	8.4	255.6	12.4	87.1	5.0	208.2	12.5	194.8	7.1	370.7	5.88	312.0	13.4
Flower Stage 15, Carpels	507.8	38.3	117.7	12.9	76.0	1.1	74.1	2.8	542.1	9.4	449.1	11.3	74.1	8.1	244.3	19.5	194.5	12.5	257.0	10.49	392.8	18.3
Flower Stage 15, Stamen	171.6	9.4	50.3	5.7	13.0	3.4	1519.4	45.6	178.4	9.5	115.9	7.8	120.1	6.2	244.3	9.4	205.6	3.6	465.8	20.38	246.6	23.5
Flower Stage 15, Petals	160.4	14.9	29.1	4.1	10.9	4.4	1039.9	43.1	85.9	4.0	53.9	3.1	88.3	14.8	368.7	5.3	254.9	3.9	875.3	46.78	274.3	10.9
Flower Stage 15, Sepals	216.7	6.2	27.5	1.1	36.9	6.6	1817.0	108.9	235.5	6.6	111.9	2.9	91.5	1.5	182.6	21.5	146.1	9.7	368.2	10.11	259.1	10.1
Flowers Stage 15, Pedicels	494.1	15.0	57.4	7.4	386.1	9.7	122.0	2.9	578.3	10.4	312.4	48.6	127.4	8.8	161.4	15.2	113.3	5.6	290.1	10.92	413.1	11.4
Pollen																						
Uninucleate Micropore	523.5	20.8	517.8	12.2	34.8	8.9	9.1	3.3	224.9	35.0	493.0	11.6	476.9	45.1	270.2	2.1	784.3	56.4	351.5	9.1	298.6	9.4
Bicellular Pollen	510.0	5.2	414.1	53.6	30.3	9.5	45.4	13.8	254.3	8.8	456.9	13.5	419.2	31.1	243.8	5.8	786.7	25.4	250.5	3.75	373.8	16.9
Tricellular Pollen	187.8	23.7	37.9	4.9	28.3	3.7	2135.8	82.2	109.4	10.2	18.8	1.3	86.2	11.9	19.9	1.1	63.7	1.1	65.0	5.59	618.9	20.7
Mature Pollen Grain	117.6	0.0	84.9	0.0	37.4	0.0	6505.7	0.0	49.0	0.0	42.1	0.0	104.8	0.0	19.3	0.0	108.0	0.0	86.5	0	697.0	0.0
Carpels																						
Stigma tissue	547.6	31.5	88.8	19.7	70.1	42.3	265.8	105.9	367.7	51.6	741.4	36.9	122.8	14.1	273.2	90.2	376.3	45.5	396.9	28.73	504.6	91.5
Ovary tissue	1064.0	164.7	196.4	26.9	241.0	20.9	162.9	56.4	594.4	148.8	953.0	118.1	171.0	14.7	515.6	138.4	321.9	86.9	639.8	74.22	794.2	118.2
Embryo development																						
Embryonic development																						
Globular - Apical	196.9	122.4	290.2	85.9	142.6	48.9	17.1	5.7	264.7	67.9	140.5	58.9	78.7	20.4	297.1	218.7	19.9	14.7	155.3	51.57	157.7	47.9
Globular - Basal	66.8	12.0	120.2	140.0	174.3	10.1	27.6	5.1	151.8	78.0	497.7	375.1	138.7	20.8	418.2	369.1	11.9	1.5	128.3	28.57	252.6	48.1
Heart - Cotyledon	140.9	89.0	1878.1	1209.4	105.7	60.7	14.5	8.5	3447.3	3271.7	890.7	671.4	74.0	28.8	208.7	142.8	4.2	1.0	128.3	36.6	3302.8	3951.0
Heart - Root	212.5	55.7	1765.1	1195.2	75.8	22.7	16.0	12.8	274.0	180.4	4418.1	2522.4	73.5	15.2	158.8	158.5	20.4	17.8	88.3	18.38	190.7	123.7
Torpedo - Cotyledon	153.7	34.5	240.0	288.1	105.9	13.2	47.2	21.5	765.1	575.1	3087.4	2470.9	75.8	42.2	616.2	618.7	13.9	9.4	127.9	19.79	216.4	146.2
Torpedo - Root	135.7	93.3	201.7	120.1	154.4	83.5	18.5	10.5	207.7	148.0	61.4	70.7	164.6	165.3	49.5	31.0	59.7	57.9	149.7	103.75	249.6	68.9
Torpedo - Meristem	321.1	243.0	310.0	236.0	99.0	42.5	15.0	4.1	335.4	162.2	3139.7	2086.5	83.1	52.5	330.7	236.6	13.5	6.6	129.7	45.36	360.6	168.4
Torpedo - Apical	209.4	71.6	1128.4	195.9	20.1	12.3	30.1	10.2	1317.2	128.4	2473.1	298.6	37.1	26.6	691.8	111.1	3.5	1.6	161.7	51.41	345.7	49.4
Torpedo - Basal	191.2	130.7	1194.6	547.3	29.7	5.0	13.1	9.4	841.4	427.8	1576.9	717.4	84.0	31.3	518.9	267.9	12.0	5.3	124.9	70.17	328.8	156.8
Seed development																						
Seed development																						
Seeds Stage 3 w/ Siliques	382.4	41.2	88.0	6.1	294.7	7.6	178.9	6.3	409.0	10.4	365.6	9.6	67.9	4.1	204.2	8.6	122.5	7.8	161.7	5.69	245.5	3.1
Seeds Stage 4 w/ Siliques	839.4	57.9	479.4	2.3	69.2	5.4	354.7	14.6	675.9	12.4	881.7	20.2	126.8	13.8	411.8	9.7	169.2	6.0	242.2	6.26	381.5	4.0
Seeds Stage 5 w/ Siliques	781.4	1.0	558.4	13.0	48.5	4.2	348.6	9.1	976.8	14.6	1221.5	53.4	91.5	4.5	448.8	27.6	158.6	13.6	186.3	4.04	468.3	15.8
Seeds Stage 6 w/o Siliques	946.8	47.1	730.0	28.7	9.4	2.4	261.9	6.7	1485.9	40.6	1556.5	89.3	104.8	3.8	695.4	41.0	115.6	8.1	121.6	7.23	647.9	20.9
Seeds Stage 7 w/o Siliques	638.4	40.1	589.4	22.0	11.4	1.4	455.7	23.1	1320.9	25.3	1247.4	34.0	111.7	0.4	746.8	33.8	83.5	4.5	119.0	7.01	476.3	22.4
Seeds Stage 8 w/o Siliques	138.0	17.6	67.4	5.0	14.2	3.4	1708.0	105.9	444.6	29.6	392.2	10.2	64.0	6.0	455.6	36.2	49.3	9.2	86.8	5.04	297.3	34.0
Seeds Stage 9 w/o Siliques	83.6	6.9	24.7	3.5	11.9	2.6	1663.8	32.6	282.6	3.7	221.5	15.4	72.6	3.8	484.2	30.6	34.9	7.5	111.1	7.17	322.3	8.1
Seeds Stage 10 w/o Siliques	77.6	6.0	13.5	9.6	13.8	3.8	1549.2	37.6	183.4	14.9	120.2	3.4	74.7	6.1	376.4	8.1	30.3	3.3	99.2	6.89	305.3	26.7
Dry seed	130.3	31.6	3.4	1.8	6.4	6.0	958.7	79.1	217.2	13.3	211.2	14.6	29.5	3.4	312.8	7.8	15.1	3.5	56.8	3.31	214.0	32.1
Imbibed seed, 24 h	456.1	8.5	97.8	24.3	6.4	2.2	1078.3	54.6	523.4	37.3	271.7	44.1	30.6	9.4	638.4	1.2	125.4	14.1	346.1	43.71	269.8	6.9

B

GENES (AGI code)

Vegetative tissues	<i>PPT1</i> At5g33320		<i>ENO1</i> At1g74030		<i>PPT2</i> At3g01550		<i>PPDK</i> At4g15530		<i>PKp1</i> At3g22960		<i>PKp2</i> At5g52920		<i>PKp3</i> At1g32440		<i>PKc</i> At5g08570		<i>PKc</i> At5g63680		<i>PKc</i> At5g56350		<i>ME4</i> At1g79750		
	E	SD	E	SD	E	SD	E	SD	E	SD	E	SD	E	SD	E	SD	E	SD	E	SD	E	SD	
Shoot																							
Hypocotyl Col-0	256.1	3.7	55.1	6.7	9.6	2.8	30.6	5.0	739.4	37.9	253.1	18.9	81.8	5.9	279.2	45.0	208.4	4.2	258.9	10.7	346.5	14.3	
Mesophyll cells	230.8	197.6	8.8	2.2	100.2	65.6	308.2	152.2	621.1	493.3	816.2	494.4	158.5	34.0	106.8	42.7	139.6	16.9	419.8	235.7	206.5	122.7	
Stem epidermis, top of stem	319.2	11.5	36.4	1.2	70.9	11.8	69.0	4.5	765.0	59.3	513.9	4.5	128.0	14.9	100.9	11.9	141.4	9.8	300.5	3.8	511.2	3.4	
Stem epidermis, bottom of stem	318.6	1.2	27.7	0.3	54.9	7.8	223.0	4.5	658.1	23.6	282.8	35.8	89.3	8.5	87.7	7.5	138.2	16.7	245.0	62.6	408.2	37.5	
Whole stem, top of stem	731.3	28.9	50.2	7.6	116.9	4.6	66.4	13.4	773.1	75.5	410.9	58.4	90.0	1.2	95.9	16.2	131.1	17.7	370.8	20.1	393.8	31.4	
Whole stem, bottom of stem	1288.9	181.3	111.0	0.3	145.6	11.1	578.0	9.6	577.9	65.2	293.7	20.3	141.1	5.1	116.2	5.4	202.9	47.2	436.9	96.4	380.6	24.9	
Xylem Col-0	254.4	32.5	25.2	3.3	10.2	1.5	116.2	1.5	494.7	25.7	156.6	6.3	82.4	5.1	127.9	1.6	158.4	13.8	291.3	12.9	571.0	32.7	
Cork Col-0	236.1	2.7	24.9	4.0	12.0	0.5	246.9	8.8	681.2	78.1	200.8	9.0	68.9	2.7	235.2	24.8	191.1	7.5	272.5	7.0	488.9	26.0	
Shoot Apex, Vegetative	808.7	13.8	303.5	11.5	65.1	8.0	5.4	2.3	681.3	33.6	632.4	2.7	85.9	3.1	267.8	3.9	142.5	6.7	245.9	3.2	432.9	6.5	
Shoot Apex, Transition	633.4	28.9	208.1	10.6	65.9	4.1	1.0	0.3	526.6	17.5	519.5	8.6	65.5	7.8	294.7	1.4	199.6	9.0	221.2	6.8	445.3	3.9	
Shoot Apex, Inflorescence	573.6	20.8	213.6	20.5	81.1	10.7	1.9	0.2	509.1	25.1	413.1	25.0	71.2	6.3	270.4	11.4	195.2	9.7	246.4	8.9	396.3	9.7	
Root																							
Root Stage III Stele	322.4	0	401.63	0	11.54	0	4.46	0	242.6	0.0	103.4	0.0	102.1	0.0	310.9	0.0	186.0	0.0	682.3	0.0	298.2	0.0	
Root Stage III Endodermis	267.43	0	469.41	0	15.97	0	4.26	0	192.2	0.0	154.9	0.0	105.3	0.0	496.1	0.0	233.3	0.0	805.6	0.0	422.1	0.0	
Root Stage III Cortex + Endodermis	475.27	0	506.28	0	8.96	0	2.9	0	209.0	0.0	201.1	0.0	119.2	0.0	370.4	0.0	219.1	0.0	619.9	0.0	415.2	0.0	
Root Stage III Epidermal Artrichoblasts	364.82	0	725.9	0	6.04	0	3.86	0	304.7	0.0	208.5	0.0	98.8	0.0	582.6	0.0	291.3	0.0	579.5	0.0	414.2	0.0	
Root Stage III Lateral Root Cap	265.21	0	421.52	0	12.74	0	13.51	0	127.8	0.0	112.8	0.0	71.2	0.0	292.2	0.0	252.3	0.0	479.7	0.0	390.8	0.0	
Root Stage II Stele	472.62	0	538.59	0	15.63	0	3.37	0	447.4	0.0	325.0	0.0	113.7	0.0	452.7	0.0	200.1	0.0	655.0	0.0	310.4	0.0	
Root Stage II Endodermis	392.03	0	629.48	0	21.63	0	3.22	0	354.4	0.0	486.8	0.0	117.2	0.0	722.3	0.0	251.0	0.0	773.3	0.0	439.4	0.0	
Root Stage II Cortex + Endodermis	696.71	0	678.93	0	12.14	0	2.2	0	385.4	0.0	632.3	0.0	132.6	0.0	539.3	0.0	235.7	0.0	595.0	0.0	432.3	0.0	
Root Stage II Epidermal Artrichoblasts	534.8	0	973.44	0	8.19	0	2.92	0	561.9	0.0	655.4	0.0	109.9	0.0	848.2	0.0	313.4	0.0	556.3	0.0	431.2	0.0	
Root Stage II Lateral Root Cap	388.77	0	565.26	0	17.25	0	10.22	0	235.6	0.0	354.5	0.0	79.2	0.0	425.4	0.0	271.5	0.0	460.5	0.0	406.8	0.0	
Root Stage I Stele	427.6	0	444.74	0	11.75	0	54.52	0	411.4	0.0	306.6	0.0	168.0	0.0	374.7	0.0	216.8	0.0	325.2	0.0	319.9	0.0	
Root Stage I Endodermis	354.69	0	519.8	0	16.25	0	52.16	0	325.9	0.0	459.3	0.0	173.3	0.0	597.8	0.0	271.9	0.0	383.9	0.0	452.7	0.0	
Root Stage I Cortex + Endodermis	630.34	0	560.63	0	9.12	0	35.55	0	354.4	0.0	596.6	0.0	196.0	0.0	446.3	0.0	255.3	0.0	295.4	0.0	445.4	0.0	
Root Stage I Epidermal Artrichoblasts	483.86	0	803.82	0	6.15	0	47.18	0	516.8	0.0	618.4	0.0	162.5	0.0	702.0	0.0	339.5	0.0	276.2	0.0	444.3	0.0	
Root Stage I Lateral Root Cap	351.74	0	466.77	0	12.96	0	165.13	0	216.7	0.0	334.5	0.0	117.1	0.0	352.0	0.0	294.1	0.0	228.6	0.0	419.1	0.0	

In silico expression analysis of genes involved in PEP and pyruvate provision to plastids of *A. thaliana*

From the segregation analysis of crosses between *cue1* and *eno1* the question arose as to why a relatively high portion of gametophytes survived albeit the mutations in *PPT1* and *ENO1* in the haploid state. There are obviously further gene functions, such as *PPT2* and/or *PPDK*, which are capable of partially compensating the lesion in *PPT1* and *ENO1* in gametophytes. In order to understand such compensational effects, we took advantage of publicly available microarray databases (e.g. <http://bar.utoronto.ca/efp/cgi-bin/efpWeb.cgi>), which provide an excellent tool to gather information on the temporal and spatial expression pattern of genes related, for instance, to PEP metabolism in plastids. Parts of this information is contained in Supplemental Figure 14 and Supplemental Table 3 (online), which show expression values of *ENO1* (At1g74030), *PPT1* (At5g33320), *PPT2* (At3g01550), *PPDK* (At4g15530), three genes encoding β or α subunits of the plastid localized PK (i.e. *PKp1* [At3g22960], *PKp2* [At1g32440] and *PKp3* [At1g32440]; Baud et al., 2007b; Lonien and Schwender, 2009), three genes encoding subunits of putative cytosolic PKs (At5g08570, At5g63680, At5g56350; Aramemnon database, Schwacke et al., 2004), and a plastid localized malic enzyme (*ME4* [At1g79750], Wheeler et al., 2005).

In generative tissues *ENO1* and *PPT1* are highly expressed (Supplemental Figure 14, E to H, Supplemental Table 3A), whereas *ENO1* expression is absent, for instance, in the leaf mesophyll (Supplemental Figure 14D, Supplemental Table 3B; compare Prabhakar et al., 2009). During early flower development (‘stage 9’ to ‘12’) *ENO1* and *PPT1* transcripts are highly abundant, whereas *PPT2* is only weakly expressed or absent (i.e. in stamen of ‘flower stage 12’ and ‘15’). The expression level of *PPDK* exhibits some fluctuations during flower development, in particular with respect to stamen and carpel specific expression. Whereas *PPDK* transcripts are highly abundant in stamen of ‘flower stage 12’ and ‘15’, they are almost absent in carpels of the same stage. In general, *PPDK* expression is absent in ‘flower stage 9’ and shows the highest levels at ‘flower stage 15’. Interestingly, *PKp1* and *PKp2* are also expressed during flower development, in particular in the reproductive organs such as stamen and carpels. Moreover, the above genes exhibit a similar overall expression pattern during embryo development with the exception of *PPDK*, which is only faintly expressed (Supplemental Table 3A).

Apart from the conversion of plastidial PEP into pyruvate by PK, an additional source for pyruvate in plastids would be the oxidative decarboxylation of malate catalyzed by plastid localized *ME4* (Wheeler et al., 2005) and the import of pyruvate by a pyruvate transporter. The transcripts of *ME4* are highly abundant both in generative and vegetative tissues (Supplemental Table 3, A and B). The expression of putative cytosolic *PK* genes can be

taken as a measure for pyruvate availability in the cytosol for import. All three *PKc* genes are expressed during flower development (Supplemental Table 3A), whereas At5g63680 shows a diminished expression during embryo development and towards the end of seed development (Supplemental Table 3A; seeds, stage 8).

A closer inspection of stromal PEP and pyruvate related gene expression, specifically during pollen development, offer a similar picture as for overall flower development (Supplemental Figure 14, Supplemental Table 3A). In contrast to *PPT1*, which constantly shows an intermediate to high transcript abundance, *PPT2* is only weakly expressed during pollen development. *ENO1* shows high transcript abundance in unicellular and bicellular pollen, but not in tricellular or mature pollen grains. In contrast, the expression of *PPDK* is almost absent in uni- and bicellular pollen, but increases to extremely high levels in tricellular and mature pollen grains. As for flower and pollen development a similar picture emerges from expression profiles during silique and seed development. *ENO1* and *PPT1* are co-expressed over a wide range of developmental stages (i.e. 'seeds stage 3' to '8'). In contrast to *PPT1*, *ENO1* expression levels drops to low levels at 'seed stages 8' to '10'. Interestingly *PPT2* is highly expressed only during the very early stage of seed development ('seed stage 3') and *PPDK* transcript abundance increases at later stages ('seed stages 8' to '10'). Furthermore, subunits of the plastid-localized PK are expressed during early to late stages of seed development. It can therefore be expected that PEP or pyruvate availability is shared between import from the cytosol and reaction sequences taking place within the plastid stroma.

The mutation of *ENO1* in the background of the *cue1* mutant not only leads to a high rate of gametophytes lethality and seed abortion, but it also affects vegetative growth and the formation of flowers (see Figure 2, main manuscript). However, growth retardation of *ccEe* plants compared to the *cue1* mutant became apparent not until plants were grown for at least four weeks on soil. Younger plantlets were not affected in shoot and root growth (compare Supplemental Figure 1B). As shown in Supplemental Figure 14C and Supplemental Table 3B, *ENO1* is expressed in most parts of the roots with the highest abundance of *ENO1* transcripts in the atrichoblasts of the rhizodermis (see also Prabhakar et al., 2009). Moreover, in contrast to *PPT2* and *PPDK*, *ENO1* and *PPT1* are also highly expressed in the shoot apex (Supplemental Figure 14B, Supplemental Table 3B) and the meristem of developing leaves (Prabhakar et al., 2009). In the *ccEe* plants, the expression of *ENO1* was severely diminished in the roots and most pronounced in the shoot apex, suggesting that a deficiency in *PPT1* combined with the reduced expression level of *ENO1* is the main reason for the observed developmental constraints of the shoot. Hence, provision of PEP to plastids in these tissues is crucial for a proper vegetative development. Growth

retardation has been observed in the *cue1*, but not in the *eno1* single mutants, suggesting that PPT1 and ENO1 can partially substitute each other during vegetative plant development. A further hint for a limitation of the shikimate pathway in the sporophyte derived from the lack of lignification of sclerenchyma cells in the inflorescence stem of *ccEe* compared to *cue1* and wild-type plants (Supplemental Figure 6). Interestingly, xylem elements appeared to be the only significantly lignified cells in *ccEe* plants. An explanation for differences in lignification of sclerenchyma cells and xylem elements might be derived from the expression profiles listed in Supplemental Table 3B. *ENO1* and *PPT1* exhibit a low and a high transcript abundance, respectively, in the whole stem, in particular at its bottom. There is also a weak expression of *PPT2* and *PPDK* in individual stem tissues (Supplemental Table 3B). A restriction of PEP provision to plastids by PPT1 and ENO1 might hence limit lignification of the sclerenchyma cells. Strikingly, in the xylem only *PPT1* and *PPDK* are significantly expressed, suggesting that lignification of xylem elements in the *ccEe* plants might derive from PEP delivered by the activity of plastid localized PPDK. However, it can not be excluded that precursors for lignin biosynthesis are transported *via* the transpiration stream.

Supplemental Table 4. Primer pairs used for qRT-PCR

AGI code	Gene name	Primer	Sequence
At5g09810	<i>Actin2</i>	sense	5' ATG GAA GCT CCT GGA ATC CAT 3'
		antisense	5' TTG CTC ATA CGG TCA GCG ATG 3'
At1g64670	<i>BDG</i>	sense	5' TAT TTG GAC CAT GTC CGT GA 3'
		antisense	5' CTT TCC TCT TGA CGC CGT AG 3'
At1g02205	<i>CER1</i>	sense	5' GTT ACC GAG AAA GGC GAT GA 3'
		antisense	5' CGA GAG AAG AAG GGA TGT GC 3'
At3g55360	<i>CER10</i>	sense	5' AAT CGG GAA TGT GTT CAG GA 3'
		antisense	5' CTT GGC AAA CCA AAC CAA AC 3'
At1g74030	<i>ENO1</i>	sense	5' TGA ACT TGT GGC TCC AAA AC 3'
		antisense	5' CTA ATA TCG CAT TAG CCC CGA GT 3'
At1g67730	<i>KCR1</i>	sense	5' CTC TCA TGG GTG CAG TTG TCT C 3'
		antisense	5' TTC TTT CTT CAT GGA GTC TTT TTG G 3'
At1g24470	<i>KCR2</i>	sense	5' CGC AGA TCG GAA TTG GAT C 3'
		antisense	5' ATA AAC TTC TTC TGC GAA GTC CG 3'
At5g57800	<i>WAX2</i>	sense	5' TGC GAG TAC ACG ATG GAG AG 3'
		antisense	5' ACA TCA ATG GCT CCA ACC TC 3'